



Statistical Analysis of Magnetic Susceptibility Variations in the Flotation Tailing of the Rudnik Mine, Republic of Serbia

Filip Arnaut^{1*} Vesna Cvetkov² Stefan Petrović² Nikola Stanković² Vladimir Simić² and Dmitry Sidorov-Biryukov²

¹ Institute of Physics Belgrade, University of Belgrade, Pregrevica 118, Belgrade, Serbia

² Faculty of Mining and Geology, University of Belgrade, Đušina 7, Belgrade, Serbia

Received 26 June 2025, in final form 10 October 2025

Mine tailings are increasingly recognized as potential valuable mineral resources. This study applies magnetic susceptibility analysis to three boreholes in flotation tailings from dumps at the Pb-Zn Rudnik Mine, Serbia. The samples were obtained over a small spatial distance (10 cm), allowing for the application of various statistical methods with the obtained dataset. The results indicate that the mutual similarity among boreholes cannot be established with statistical significance; however, certain zones between boreholes exhibit some similarities. These variations are attributed to anthropogenic deposition, where local materials were intermixed and arbitrarily deposited during mining and processing, preventing clear statistical correlations. The study identifies key zones of interest in all three boreholes for further geochemical and mineralogical investigations.

Keywords: Spatial analysis, magnetic susceptibility, anthropogenic deposition, geostatistics, tailings, tailing recycling

1. Introduction

Recent advancements in the field of mining have led to the growing recognition of mining tailings as valuable mineral resources (Jawad and Randive, 2021). These by-products once considered environmental liabilities (Barraza et al., 2024), now offer new opportunities for economic gain, providing supplementary revenue streams for mining companies. In particular, flotation tailings are increasingly seen as key components in the recycling and reuse of materials, which in turn reduces the need for new resource extraction and contributes to environmental conservation. This shift in perspective presents a range of benefits, including economic growth, job creation, and technological advancements in the recycling sector, making the utilization of mining tailings a promising avenue for sustainable development.

Flotation tailings are a specific type of mine tailings generated from the flotation process, which is a chemical method used to separate hydrophobic (water-repellent) materials from hydrophilic (water-attracting) materials

(Jain et al., 2025). The term "heavy metals" denotes metals and metalloids (Tchounwou et al., 2012) associated with environmental contamination and potential toxicity to humans and the local ecosystem (Jaishankar et al., 2014 Briffa et al., 2020). The mining industry produces tailings especially inclined to elevated concentrations of heavy metals, which may result in adverse health outcomes if these metals infiltrate the human body (Liu et al., 2023). The environmental impact of tailings can accumulate over time or manifest abruptly due to external triggers such as earthquakes or flooding (Su et al., 2024), which can lead to larger environmental problems. Numerous environmental contaminations resulting from tailing storage have been documented in the Republic of Serbia, including Valja Fundata (Majdanpek) in 1974, Šaški potok (Majdanpek) in 1996, and Stolice (Krupanj) in 2014 (Nišić et al., 2024).

As the technology for refining and reusing material from tailings advances, tailings are increasingly regarded not as waste but as a mineral resource that can be further utilized (Cacciuttolo et al., 2023). Innovative methods for assessing heavy-metal concentration in materials have been established, notably the magnetic susceptibility (MS) technique, where either volume- specific MS (κ) is measured or mass- specific MS is measured (χ). In the last twenty years, laboratory measurements of MS, typical for paleomagnetic investigations, have been utilized in ecology, particularly for identifying and assessing the spatial distribution of (anthropogenic) heavy metals (Lecoanet et al., 1999; Petrovský et al., 2000; Karimi et al., 2011; Wang, 2013; Brempong et al., 2016; Oudeika et al., 2020). Magnetic susceptibility depends on the geochemical and mineralogical composition of the material being studied (Frances et al., 2017), particularly the presence of iron-rich magnetic minerals. Magnetic minerals are characterized by their affinity for other elements, especially heavy metals (Bityukova et al., 1999; Boyko et al., 2004; Hanesch and Schloger, 2005; Kim et al., 2010; Salehi et al., 2013; Zawadzki et al., 2015; Brempong et al., 2016; Jaffar et al., 2017; Vasiliev et al., 2020). Assessments of MS in mining tailings have demonstrated a robust positive correlation between heavy metal presence and elevated MS values (Jordanova et al., 2013; Gómez-García et al., 2015; Lam et al., 2020). In contrast to traditional methods necessitating specialized sample preparation and extended timeframes for results, laboratory measurements of MS demand no special sample preparation and provide rapid results at a considerably reduced cost (Hanesch and Scholger, 2002; D'Emilio et al., 2010). Moreover, the samples remain unaltered following MS measurements and are suitable for subsequent geochemical (such as X-ray fluorescence analysis, instrumental neutron activation analysis and inductively coupled plasma mass spectrometry etc.) or mineralogical examinations (such as optical and electron microscopy (SEM/EDS), FTIR spectroscopy etc.). This investigation can thus function as a rapid and effective proxy method for evaluating environmental conditions and identifying primary sources of heavy metals (Morales et al.,

2016; Yurtseven-Sandker and Cioppa, 2016; Petrovský et al., 2000; Wawer, 2020; Jabłońska et al., 2021). The application of suitable statistical methods enables the acquired data to serve as a semi-quantitative instrument for characterizing mining tailings (Lam et al., 2020). The initial study of the correlation between x and heavy metal concentration in flotation tailings from the Rudnik mine was done utilizing samples obtained from 16 depth intervals, reaching a maximum depth of 8 meters (Abramović et al., 2022). Geochemical analysis indicated that increased x values were associated with samples containing Fe ($r=0.891$), Co ($r=0.875$), Cr ($r=0.562$), As ($r=0.572$), and Cu ($r=0.451$). A strong correlation was also identified with Bi ($r=0.841$) (Abramović et al., 2022).

The objective of this research is to statistically analyze the x values acquired from three boreholes, assess the degree of similarity among the materials from these boreholes, identify zones of interest (ZI) for further analyses, including geochemical and mineralogical tests, and evaluate the applicability of various time-series analysis methods on spatially dependent data. All previously mentioned objectives, except the final one, pertain to conventional exploration techniques that utilize statistical methods to acquire supplementary information from the measured data. The final objective, which involves the application of time-series analysis methods, was examined in this research paper to determine which methods yield novel insights into univariate, spatially-dependent data.

2. Methods and data

2.1. Characteristics of the flotation tailings of the Pb-Zn Rudnik mine

The flotation tailing is located near the active Rudnik mine in central Serbia (Fig. 1b). The Rudnik mine has been an important regional source of polymetallic ore, producing ~13 million metric tons of Zn, Pb, Cu, and Ag to date (Jelenković et al., 2008; Popović and Umeljić, 2015).

The polymetallic ore is hosted within over 90 ore bodies, associated with two main geological units: the contact metamorphic rocks and the extensive volcanic as well as shallow intrusive facies of quartz latite (Cvetković et al., 2016; Petrović et al., 2024).

The ore bodies are composed of sulfide minerals, with pyrrhotite being the most abundant. Other major ore minerals include sphalerite, galena, and chalcopyrite, while gangue minerals such as arsenopyrite and pyrite are also present (Stojanović et al., 2016). The metal content in the ore varies significantly, with Pb ranging from 0.94 to 5.66 wt%, Zn from 0.49 to 4.49 wt%, Cu from 0.08 to 2.18 wt%, and Ag ranging from 50 to 297 µg/g (Stojanović et al., 2018).

This study focuses on investigating flotation tailing of the Rudnik mine (Fig. 1). Tailing formation at the Rudnik mine began in 1953 due to the flotation process used to produce concentrates of K/PbS , $K/CuFeS_2$, and K/ZnS . Over the course of mining and flotation operations, more than 11 million tons (approximately 7 million m^3) of flotation by-products have been generated and deposited in the tailings. As a result, the flotation tailings now form an oval shape, stretching in a southeast-northwest direction, covering an area of about 41 hectares and reaching depths of up to 40 m (Fig. 1c).

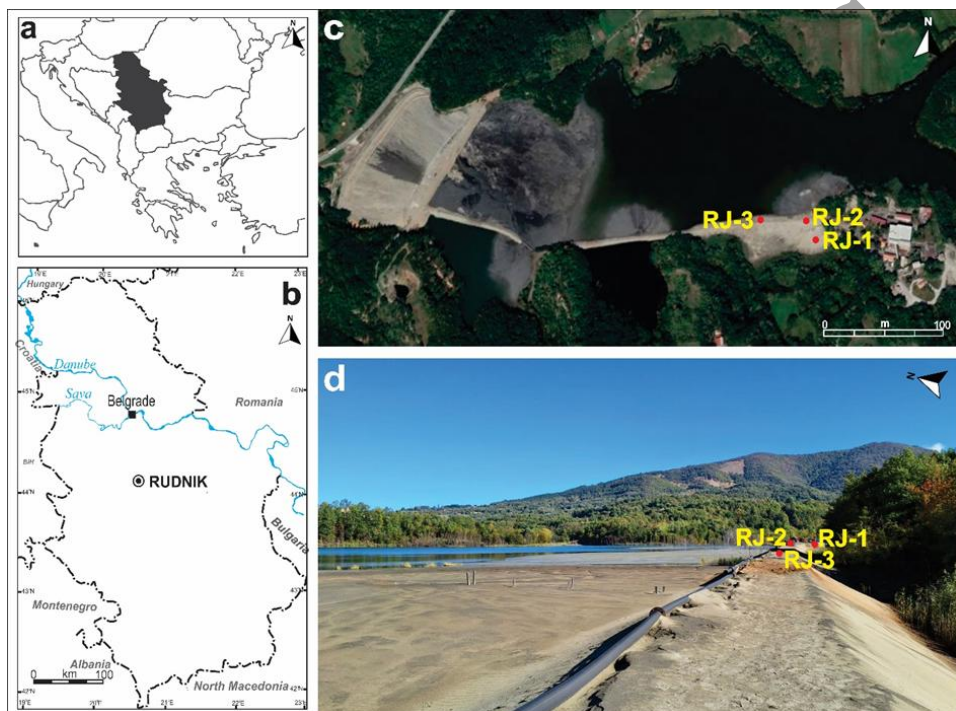


Figure 1. (a) Location of the Republic of Serbia within SE Europe; (b) The location of the Rudnik mine in the Republic of Serbia; (c) Satellite image of the spatial distribution of the three boreholes (RJ-1, RJ-2 and RJ-3); (d) Field photograph of the mine tailing site with the place of the three boreholes.

Internal, unpublished investigations conducted at the Rudnik mine indicate that the flotation tailings are mainly composed of fine-grained material (<0.074 mm) (Obrenović et al., 2025). The tailings are mainly composed of aluminosilicate minerals, such as quartz and feldspar, which together make up over 60% of the material. Additionally, smaller quantities (5–10%) of clay minerals are present, along with trace amounts of residual Pb, Zn, Cu, and Fe, collectively accounting for up to 1% of the tailings. This composition reflects the mineralogical characteristics of the ore and the flotation process, which concentrates the valuable metals.

Samples for this study were collected from three boreholes, designated RJ-1, RJ-2, and RJ-3, located at the northwestern boundary of the flotation tailings pond (Fig. 1d). The boreholes were drilled during the summer of 2024 in the drier section of the pond, with the first and second boreholes spaced 30 m apart, and the second and third boreholes 50 m apart. The first borehole is situated in the older section of the pond, while the other two are located along the embankment formed by the deposition of tailings from the hydrocyclone. Both the older section and the embankment contain recent material up to 2 meters thick, beneath which lies flotation waste material. The total core lengths for the three boreholes were 11.9 m, 13.4 m, and 14.6 m, respectively. Samples were collected from each borehole in 10 cm increments, resulting in a total of 356 samples from the three boreholes.

2.2. Magnetic susceptibility sampling and measurements

The sampling of the tailing embankment at Rudnik was conducted using exploratory boreholes, from which samples were extracted from the core at 10 cm intervals. The high-resolution samples facilitated the collection of extensive data for MS measurements, thereby allowing for precise spatial tracking of changes in the tailing material. Subsequent to the systematic field sampling, the samples collected from the Rudnik tailing were initially dried under ambient laboratory conditions for several weeks, after which all of the samples were packed in 12 cm³ Bartington MS2B sample containers for subsequent processing. The second step involved obtaining mass measurements using the Radwag AS 220.R2 Plus laboratory scale to enable calculations of χ . χ measurements were conducted using the Bartington MS2B sensor in conjunction with the Bartington MS3.

χ measurements of empty sample containers were conducted on 10 randomly selected containers from the entire collection, which were utilized to calculate the apparent susceptibility of the samples by subtracting the measured apparent MS from that of the empty sample container. The final χ and κ were computed from the sample mass apparent susceptibility value and either the mass susceptibility coefficient or the volume susceptibility coefficient, as determined according to the manufacturer's guidelines (Bartington, 2008). In this research only the χ was utilized.

2.3. Statistical methods

This research employed various statistical methods, including standard techniques such as descriptive statistics, distributions, and correlations, as well as statistical tests like the Kolmogorov-Smirnov test and time-series analysis methods which were applied to spatial data to determine if they provide any potential supplementary insights.

The employed descriptive statistics consist of standard metrics for a dataset, including the computation of the mean, median, maximum and minimum values, variance, coefficient of variation (CV), skewness, and kurtosis. Analyzing data distributions provides insights into the variability of the dataset, including the identification of potential outliers and the visualization of the skewness and kurtosis of a given dataset's distribution. In addition to the data distributions, the cumulative distribution function (CDF) was presented to visualize the data percentiles and facilitate the interpretation of the Kolmogorov-Smirnov test.

Furthermore, this research utilized Hartigan's dip test (Hartigan and Hartigan, 1985) to analyze the data regarding modality type. The dip test was employed to determine the distribution type for each borehole, specifically determining whether the χ values are unimodal or bimodal. The dip test was conducted using the *dip test* library in Python, which calculates two values: the dip test statistic and the corresponding p-value. The dip test statistic quantifies the extent of deviation from unimodality, while the p-value evaluates the statistical significance concerning the null hypothesis of unimodality.

Correlation coefficients (CCs) are effective tools for evaluating the strength and direction of the relationships between two datasets. This research primarily utilized two correlation coefficients: Pearson's correlation coefficient (PCC) (Rodgers and Nicewander, 1988) and Spearman's correlation coefficient (SCC) (Zar, 2005). The PCC is the most widely employed CC, quantifying the strength and direction of an assumed linear relationship between two variables. PCC presumes that the datasets exhibit a linear relationship and that both variables follow a normal distribution. Conversely, SCC is a non-parametric CC that neither assumes normality of the variables nor the nature of the relationship between them. This research employed both CCs and conducted a comparative analysis between them. Given that the two employed CCs operate under different assumptions, they will be used initially to examine the nature of the relationship between the individual boreholes and to assess the strength and direction of that relationship. If the two CCs exhibit divergent values, the SCC will be prioritized and carry greater significance (see e.g., Schober et al., 2018).

The Kolmogorov-Smirnov (KS) test is a statistical method that compares a dataset's distribution to a theoretical distribution (one-sample KS test) (Cardoso and Galeno, 2023) or evaluates whether two datasets derive from the same distribution (two-sample KS test). The KS test was employed to assess whether the distribution of χ data conforms to a normal distribution (Naimi and Ayoubi, 2013; Ayoubi and Mirsaidi, 2019). This research employed the two-sample KS test in two capacities: first, to assess whether individual two boreholes originate from the same distribution, and second, to determine if a

specific layer within a borehole derives from the same or a different distribution compared to adjacent layers.

Time-series analysis methods comprise a set of statistical techniques designed for datasets collected over time, typically under the assumption that measurements were taken at uniform intervals (Velicer and Fava, 2003). Time-series analysis includes a variety of statistical techniques, including stationarity tests, various visualizations, transformations, and additional methods that facilitate the analysis of time-dependent data (for reference on different time-series analysis and forecasting techniques refer to Hyndman and Athanasopoulos, 2021). This research utilized stationarity tests, first difference analyses, and cumulative sum visualizations on spatially-dependent data.

Stationarity tests are employed in time-series analysis to determine whether the dataset exhibits consistent statistical properties over time, specifically a stable mean and variance. The purpose of employing stationarity tests for spatial data is to determine whether the dataset exhibits consistent statistical properties across a spatial dimension, specifically depth in this question. Stationarity testing was performed using two methods: the Augmented Dickey-Fuller (ADF) test (Dickey and Fuller, 1979; Dickey and Fuller, 1981) and the Kwiatkowski-Phillips-Schmidt-Shin (KPSS) test (Kwiatkowski et al., 1992). In interpreting the ADF test, if the test statistic is lower than the critical value at the specified significance level (e.g., 0.05), the null hypothesis should be rejected in favor of the alternative hypothesis, signifying that the data is stationary. If the test statistic exceeds the critical value, the null hypothesis cannot be rejected, indicating that the data is non-stationary. In the KPSS test, the null hypothesis suggests that the data exhibits stationarity. If the test statistic is less than the critical value at a significance level of 0.05, the null hypothesis remains, suggesting that the data is stationary. Should the test statistic exceed the critical value, the null hypothesis must be rejected in favor of the alternative hypothesis, indicating that the data is non-stationary. The dual testing approach was chosen because the majority of researchers (66.5%) conduct only a single test and exhibit caution when confronted with inconclusive results (Lyocsa et al., 2011).

The first and second differences of time-dependent datasets are commonly employed transformations to achieve stationarity when the original dataset is non-stationary. The primary objective of the first difference of a dataset is to de-trend, meaning to subtract any existing trend, thereby isolating only local variations. The first-differenced dataset typically consists of data that oscillates around the mean value, exhibiting only localized and rapid fluctuations. This research examined the efficacy of the first difference transformation and its corresponding representation for improving spatially-dependent data, specifically χ borehole data, and assessed whether they yield additional insights beyond the original data.

Analogous to the first difference transformation and visual representation, the cumulative sum (CUSUM) graph was utilized to assess its advantages for spatially-dependent datasets. The CUSUM graph is frequently used in quality control procedures to monitor the underlying mean of the process. The primary characteristic of CUSUM graphs, as opposed to other quality control graphs, is their capacity to swiftly identify minor changes (Nenes and Tagaras, 2006). The CUSUM graph illustrates the deviation of each data point in a sequence from a reference or predetermined value, specifically the overall mean of the dataset. The interpretation of the CUSUM graph is straightforward; stable values indicate a stable underlying process, while positive or negative values reflect upward or downward trends in the original dataset. Sudden fluctuations raise notion of a local anomaly or a significant deviation from the overall mean of the original dataset. In this study, the CUSUM graph was similarly evaluated for its applicability to spatially-dependent datasets, specifically χ borehole measurements.

The primary objective of employing time-series analysis methods on spatially-dependent data is to determine whether methods designed for time-series datasets can yield novel insights into spatial data as well. In time-series analysis, the methodologies employed in this research require that temporal observations be gathered at uniform time intervals. This research collects χ data at uniform spatial intervals of 10 cm, facilitating comprehensive data sampling for qualitative application of time-series analysis techniques to spatially-dependent data.

3. Results

3.1. Measurement validation

Measurement verification was conducted via two methods. Initially, after every 10 measurements, corresponding to 1 meter, the repeated measurements of the calibration sample χ were conducted (Fig. 2a). Additionally, every 10th measurement was repeated three times, and the percentage difference was computed and presented (Fig. 2b-d). The manufacturer's calibration value indicates 3133×10^{-5} SI at a temperature of 22 °C. The calibration check was conducted 12 times for boreholes RJ-1 and RJ-2, and 15 times for borehole RJ-3 during the measurement process. All three boreholes exhibit minimal deviations from the calibration sample, on the order of 10⁻² percent. Repeated measurements for all three boreholes exhibit percentage discrepancies under 1.3% (Fig. 2 b, c, d). The dual validation of samples rendered the measurements accurate and appropriate for subsequent data processing and analysis.

The final dataset from the three tailing boreholes at the Rudnik mine comprised a total of 356 measured MS data points. The initial borehole RJ-1 encompasses measurements from 1.3 m to 12 m, the second ranges from 0 m

to 11.1 m, and the third extends from 0 m to 14.6 m. All three boreholes were subjected to statistical tests and time-series analysis methods, resulting in their depths being standardized. Each borehole for data analysis begins at 1.3 meters and concludes at 11.1 meters, yielding 99 data points per borehole, totaling 297 data points across all three boreholes. The decision to eliminate certain data from either the surface or deeper layers was made to ensure uniform starting and ending depths for all three boreholes, thereby enabling consistent data analysis across them.

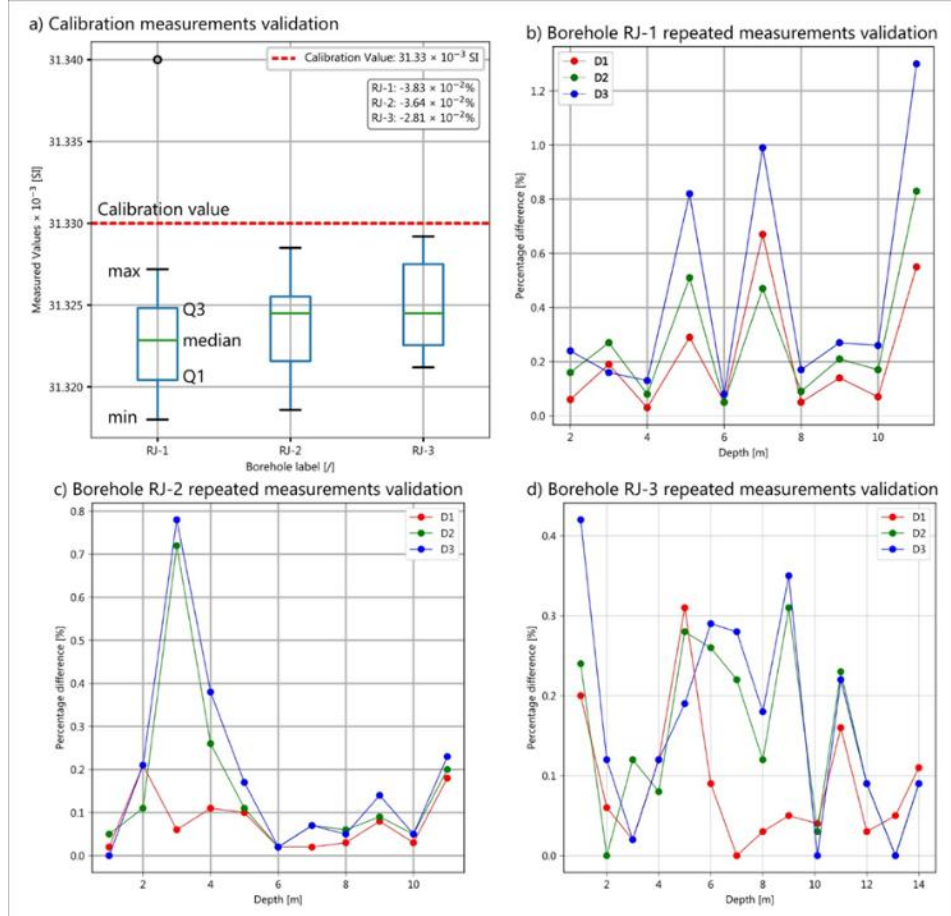


Figure 2. (a) Validation of measurements with the calibration sample; (b) Repeated calibration measurements for borehole RJ-1; (c) Repeated calibration measurements for borehole RJ-2; (d) Repeated calibration measurements for borehole RJ-3; D1- Percentage difference of the first repeated measurement against the first measurement; D2- Percentage difference of the second repeated measurement against the first measurement; D3- Percentage difference of the third repeated measurement against the first measurement.

3.2. Determination of potential zones of interest

For this research, zones of interest were delineated as areas where χ exhibits variations distinct from prior and subsequent measurements. Fig. 3 illustrates four zones of interest (ZI) across all three boreholes. Borehole RJ-1 reveals a singular zone of interest located at a depth ranging from 4 to 6 meters derived based on a visual interpretation. Measurements taken prior to the 4-meter mark indicate a minor downward trend, followed by a slight upward trend in the 4 to 6-meter range, featuring a significant outlier just before the 6-meter mark. χ values beyond the 6th meter mark exhibit a fluctuating pattern characterized by a relatively rapid alternation between increased and decreased χ values. The highlighted area is compelling due to the sharp outlier that begins prior to the 6th meter, potentially indicating a notable alteration in χ properties within the specified layer, while the χ exhibits a subtle increasing trend from the 4th meter onward.

Borehole RJ-2 exhibits two zones of interest, the first located between the 4th and 6th meters, and the second beyond the 10-meter mark. Analogous to RJ-1 at the fourth meter, χ exhibits an upward trend with two discernible outliers. The second ZI exhibits a noticeable increase in χ following the 10th meter. The measurements between the two ZI exhibit relatively stable properties, with a significant outlier being the lower χ value at approximately the 9-meter mark.

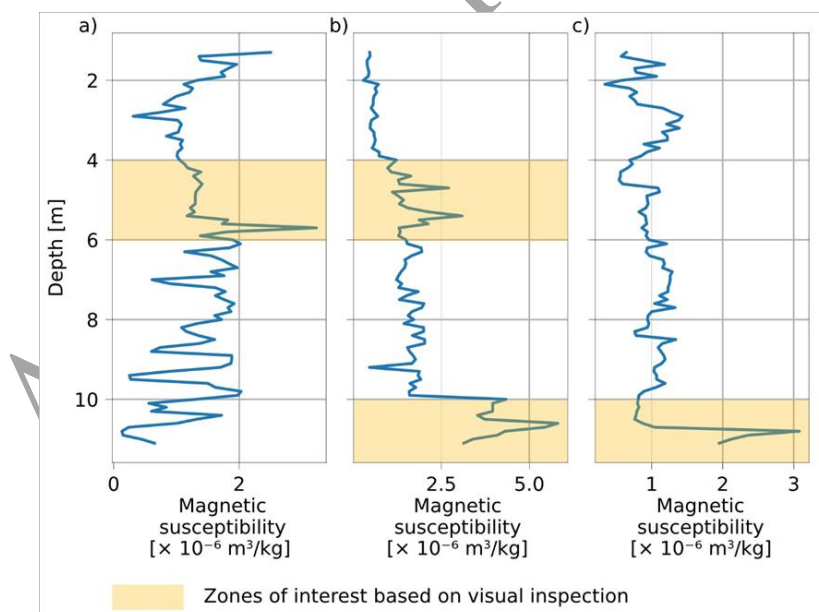


Figure 3. Identification of zones of interest based on mass magnetic susceptibility measurements; (a) Borehole RJ-1; (b) Borehole RJ-2; (c) Borehole RJ-3.

Borehole RJ-3 displays a single ZI, similar to borehole RJ-1 which also displays only one ZI. The difference between RJ-3 and RJ-1 is that within RJ-3 the ZI is located at a depth of 10 meters as opposed to RJ-1 where that ZI is located between the 4th and 6th meter. The measurements of χ prior to the 10th meter exhibit relatively stable statistical characteristics with the exception being the increase and subsequent decrease in χ values between the 2nd and 4th meters, which are deemed to be slight local fluctuations and not interpreted as a rapid deviation of MS

3.3. Intra-borehole statistical analysis

Descriptive statistics have been calculated and analyzed for each of the three boreholes (Table 1). Fig. 3 illustrates that the highest values of χ are found within the material deposited at the location of borehole RJ-2. Descriptive statistics confirm that borehole RJ-2 exhibits the highest mean, median, maximum value, range and variance. The CV most effectively illustrate the disparities in χ variations among the three boreholes, with borehole RJ-2 exhibiting the highest CV at approximately 69%, while boreholes RJ-1 and RJ-3 display relatively similar CVs of 40% and 35%, respectively (Table 1).

Table 1. Descriptive statistics of mass magnetic susceptibility measurements.

Parameter/ Borehole	RJ-1	RJ-2	RJ-3
Mean [$\times 10^{-6}$ m ³ /kg]	1.32	1.63	1.03
Median [$\times 10^{-6}$ m ³ /kg]	1.31	1.47	0.96
Min [$\times 10^{-6}$ m ³ /kg]	0.13	0.29	0.34
Max [$\times 10^{-6}$ m ³ /kg]	3.23	5.81	3.08
Range [$\times 10^{-6}$ m ³ /kg]	3.10	5.52	2.74
Variance [$\times 10^{-6}$ m ³ /kg]	0.27	1.26	0.13
CV [%]	0.40	0.69	0.35
Skewness [%]	0.11	1.55	2.52
Kurtosis [%]	0.98	2.47	10.73

Descriptive statistics revealed the difference and similarities of the χ values among the three boreholes, while the distributions illustrated in Fig. 4 provide additional insight into these differences and similarities. Distributions of boreholes RJ-1 and RJ-2 exhibit visual similarities, each displaying two distinct peak values up to the first two meters indicating possible multimodality. Borehole RJ-3 exhibits the highest skewness, as indicated by the descriptive statistics and with a kurtosis parameter approximately five times greater than that of the second highest, RJ-2 (Table 1). Hartigan's dip test was utilized to assess the modality (unimodality or bimodality) of the

borehole data distributions. The dip test results indicated that boreholes RJ-1 and RJ-3 are unimodal. Borehole RJ-2 exhibited a bimodal distribution, indicating two mode values, thereby emphasizing its distinctions from boreholes RJ-1 and RJ-3. The disparity between the CDFs of RJ-1 and RJ-2 is more evident, as the horizontal spread between RJ-1 and RJ-3 is similar, while RJ-2 exhibits a significantly greater horizontal spread. In both RJ-1 and RJ-3, a limited number of data points are outliers (2 (above $2 \times 10^{-6} \text{ m}^3/\text{kg}$) and 4 (above approx. $1.9 \times 10^{-6} \text{ m}^3/\text{kg}$), respectively), whereas RJ-2 exhibits a greater quantity of data points in the higher percentile of χ values (approx. 14)

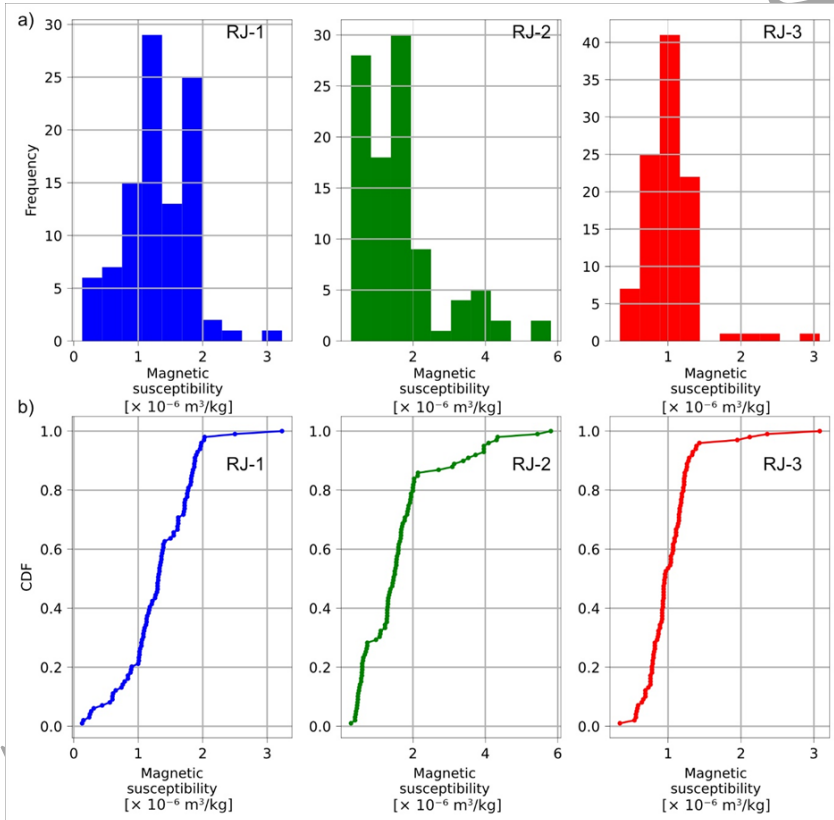


Figure 4. (a) Magnetic susceptibility distributions for boreholes RJ-1, RJ-2 and RJ-3; (b) Magnetic susceptibility cumulative distribution functions for boreholes RJ-1, RJ-2 and RJ-3.

Subsequent analysis incorporated the KS test (Table 2), which aimed to determine the extent of similarity among the three boreholes, specifically identifying which boreholes originate from a similar data distribution. The results indicated that boreholes RJ-1 and RJ-2 are mutually comparable, whereas both RJ-1 and RJ-2 are distinct from borehole RJ-3. If only the KS test is interpreted the interpretation would indicate that the material in

boreholes RJ-1 and RJ-2 are somewhat comparable, whereas borehole RJ-3 is entirely dissimilar to the other two.

Table 2. Kolmogorov-Smirnov (KS) test for boreholes RJ-1, RJ-2 and RJ-3.

Borehole	KS Statistic [l]	KS p-value [l]
RJ-1 vs RJ-2	0.17	1.08×10^{-1}
RJ-1 vs RJ-3	0.45*	$1.36 \times 10^{-9*}$
RJ-2 vs RJ-3	0.55*	$7.26 \times 10^{-14*}$

*Significant differences

Subsequent analysis involved the utilization of CCs, specifically the PCC and SCC, to assess the degree of similarity between the boreholes if the two coefficients yield divergent outcomes. Fig. 5 presents correlation matrices for both PCC and SCC pertaining to the three boreholes. The results for the three boreholes demonstrate possibly a non-linear relationship, as evidenced by the significant disparity in PCC and SCC values. Furthermore, the SCC indicates that the CCs among the boreholes are negligible to weak, with the highest CC of only 0.11 observed between RJ-2 and RJ-3.

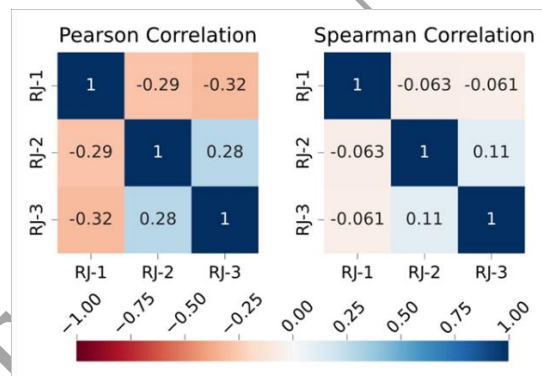


Figure 5. Pearson's and Spearman's correlation coefficients for boreholes RJ-1, RJ-2 and RJ-3.

Finally, all boreholes underwent stationarity testing (Table 3), revealing that boreholes RJ-1 and RJ-3 are stationary according to both the ADF and KPSS tests, whereas borehole RJ-2 exhibits non-stationary statistical behavior, indicating that the mean and variance are not constant with depth.

Table 3. Stationarity testing of the boreholes.

Borehole	ADF TS	ADF CV [5%]	Interpretation	KPSS TS	KPSS CV [5%]	Interpretation
RJ-1	-5.03		Stationary	0.25		Stationary
RJ-2	-1.62	-2.89	Non-stationary	1.16	0.463	Non-stationary
RJ-3	-3.71		Stationary	0.43		Stationary

3.4. Inter-borehole statistical analysis

The intra-borehole statistical analysis involved comparing the identified ZI with the layers preceding and succeeding them. Fig. 6 illustrates the original data, the first difference, and the CUSUM of the χ data for all three boreholes. The first-difference data indicates that the highlighted ZI exhibit the greatest variation within a specific borehole, underscoring that the most significant variation across all borehole data occurs in this particular zone. The CUSUM data indicates that for borehole RJ-1, a significant mean change occurs twice within the ZI: first at the 4-meter mark, where a general downward trend transitions to a constant trend, and subsequently just before the 6-meter mark, where the trend shifts to a generally increasing trajectory. Borehole RJ-2 presents a simpler scenario with two change points: one at the 4-meter mark and the other at the 10-meter mark, both situated at the starting point of the ZI. The situation for borehole RJ-3 is relatively more complex. The change-point associated with the ZI indicates a transition from an upward to a downward trend; however, within the ZI, there exists another, more significant change-point. The CUSUM graph for RJ-3 also exhibits local variation in χ .

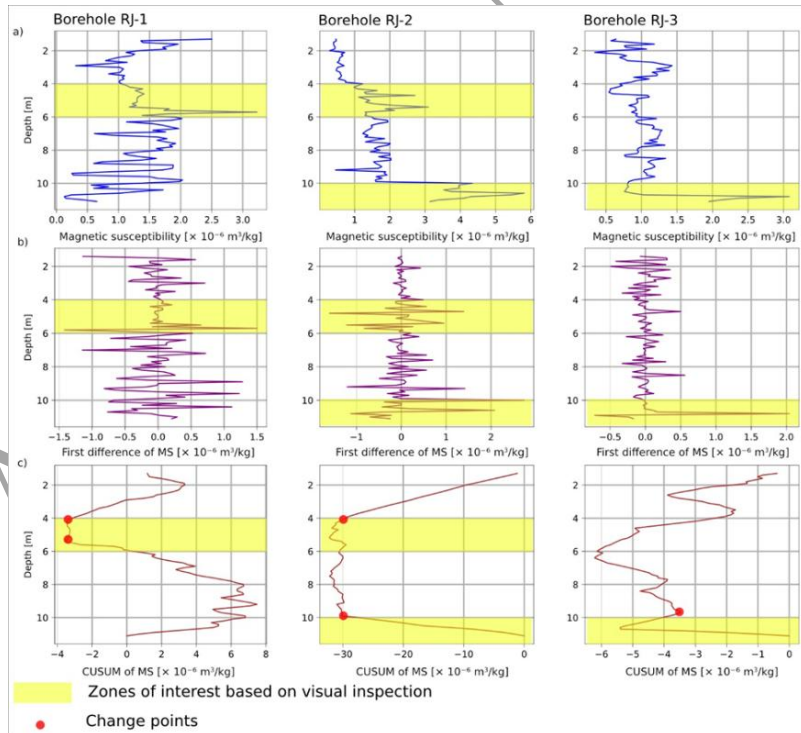


Figure 6. (a) Original magnetic susceptibility data; (b) first difference of the magnetic susceptibility data and (c) cumulative sum (CUSUM) of the magnetic susceptibility data.

The intra-borehole analysis of the ZI layers, along with the adjacent layers, specifically the preceding and succeeding MS layers, is presented in Table 4. The ZI in RJ-1 is markedly different from both the preceding layer (2-4 meters) and the subsequent layer (6-8 meters) according to the KS test. The borehole RJ-2 indicates that the ZI layer, extending from 4 to 6 meters, is distinct from the preceding layer (2-4 meters) but not dissimilar to the subsequent layer (6-8 meters). The RJ-3 borehole indicates that the ZI layer is not statistically distinct from the preceding layer. For the second ZI of borehole RJ-2 and the only ZI of borehole RJ-3, comparison to the subsequent deeper layer was not possible as the layer in question represented the deepest in the provided dataset.

Table 4. Intra-borehole analysis results.

Borehole	Zone	KS statistic	KS p-value
Layer before			
RJ-1	1	0.75	9.55E-06
RJ-2	1	1.00	1.45E-11
RJ-2	2	0.60	1.12E-03
RJ-3	1	0.35	1.75E-01
Layer after			
RJ-1	1	0.65	2.70E-04
RJ-2	1	0.4	8.11E-02

4. Discussion and verification with lithological data

The analysis was conducted in a "blind" manner, relying solely on χ data without incorporating additional borehole information such as lithological data. Consequently, verifying the results with lithological data post-analysis serves as an important validation and correlation process (Fig. 7).

In borehole RJ-1, the zone of interest is situated between 4 and 6 meters, where a maximum value of χ was identified. The maximum value pertains to gray sands, which are differentiated from the preceding layer of gray-red sands and the subsequent layer of gray, slightly clayey sands. The KS test was employed to analyze the layer in question, revealing its distinction from both the preceding and subsequent layers, a finding supported by the lithology data. The CUSUM graph for the ZI in RJ-1 demonstrates relatively stable values, suggesting stability within the ZI until the peak value, approximately 5.7 meters in depth. The CUSUM graph after 5.7 meters in depth exhibits an upward trend that persists until the 10th meter, where it transitions to a downward trend upon encountering gray clayey sands.

The χ values in RJ-2 exhibit relatively stable values until the 4th meter, where a slight increase and two distinct peaks are observed. The peaks

constitute a section of the gray, slightly clayey sand layer, which exhibits distinct lithological characteristics compared to the preceding gray-red clayey sand layer and the subsequent gray sand layer. The CUSUM graph is verified, indicating stability at the 4-meter mark, which persists until the 10-meter mark. The KS test indicated that the initial ZI in RJ-2 differed from the preceding layer but not from the subsequent layer. The overall CUSUM value decreases until the 4-meter mark, after which it relatively stabilizes until the 10-meter mark. In contrast to RJ-1, the 4-6 m ZI in RJ-2 shows no change point detection by the CUSUM test, likely due to relatively higher variability of the data within the 4-10 m depth interval. The overall mean of the function is not significantly different between the 4-6m ZI in RJ-2 and the subsequent 6-10m layer, which may explain why the KS test indicated that the initial ZI in RJ-2 differed from the shallower layer but not from the deeper layer. The second ZI in borehole RJ-2 is indicated from the 10-meter mark and exhibited a difference from the preceding layer according to the KS test. The shift from gray sands to red-gray, slightly clayey sands exhibited an elevation in χ and a changepoint in the CUSUM graph. Likewise, another interesting ZI can be examined prior; however, it was excluded from this analysis due to its relatively thin layer, specifically the red sands between 9.1 and 9.2 meters, where the χ significantly decreases in value.

Borehole RJ-3 exhibits localized fluctuations in the CUSUM value, as previously noted, which are attributed to red and red-gray sands. Subsequent to the initial minor fluctuations, the χ values remain relatively stable, exhibiting no abrupt increases or decreases. Following the 10-meter mark, similarly to borehole RJ-2, the χ values exhibit a sudden increase (Fig. 7.b,c), which can be attributed to the deeper layers of gray sands. This layer was not significantly different from the preceding layer according to the KS test; however, it exhibits some interesting properties for further research.

The statistical analysis conducted in this research paper yielded inconsistent results that were challenging to interpret. The analysis of ZI indicates that the three boreholes may exhibit similarities, as both RJ-1 and RJ-2 show elevated values at the 4–6-meter depth, and RJ-2 and RJ-3 at the 10+ meter depth. Subsequent analysis utilizing descriptive statistics and distributions revealed more differences than similarities, particularly evident in the skewness and kurtosis parameters, and notably in Hartigan's dip test, which indicated different results for RJ-1 and RJ-2 despite their apparent similarity.

The bimodality of the RJ-2 borehole may be associated with two ZI's, both exhibiting elevated χ values, signifying an increase in heavy metal content within the specified layer. The MS method is limited in its ability to differentiate the composition of the two ZI's, necessitating further geochemical or mineralogical analysis for that task.

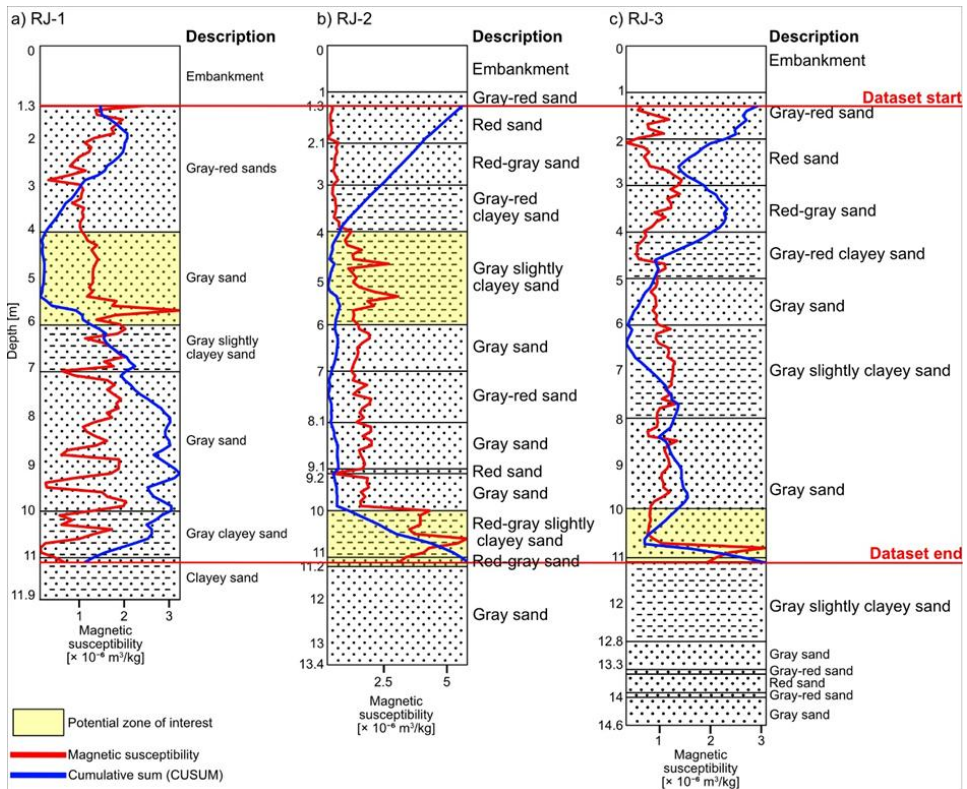


Figure 7. Verification with lithological data; (a) Borehole RJ-1; (b) Borehole RJ-2 and (c) Borehole RJ-3

The KS test was employed to compare the χ values among the three boreholes to determine whether they originate from the same distribution i.e., population. The material comprising the three boreholes originates from the same spatial area, specifically from the Rudnik mine; however, the deposition of this material is the primary focus of this research. Based exclusively on the descriptive statistics and distributions, it can be assumed that RJ-1 and RJ-3 are comparable, while RJ-2 is the outlier. However, the KS test yielded contrasting results, indicating that both RJ-1 and RJ-2 are dissimilar to RJ-3, while RJ-1 and RJ-2 are mutually similar.

The application of the PCC and SCC to establish a similarity index between boreholes revealed minimal correlation values in both instances, thereby indicating a low spatial correlation among the boreholes. Moreover, the calculation of both the PCC and SCC reveals that, due to the differing values obtained, a strictly linear relationship cannot be assumed. This is expected, as the PCC solely quantifies the intensity of the linear relationship between two variables. The remaining possibilities are that the boreholes

display a non-linear correlation or that there is minimal to no correlation between them. Considering the characteristics of the deposited material, the latter interpretation appears more credible- indicating an absence of significant correlation between the materials in the examined boreholes.

The earlier discussion illustrates challenges in applying geological or statistical interpretations to anthropogenically deposited materials such as mine tailings where the deposited material is not formed through natural geological processes yet it is a result of human mining activities. The analysis indicates that there is minimal confidence in concluding that any of the three boreholes exhibit overall similarities. Certain potential ZI's may be locally perceived as comparable between boreholes, exemplified by RJ-1 and RJ-2, as well as RJ-2 (second ZI) and RJ-3; however, the overall analysis suggests that the interpretation of mutual similarity among boreholes is minimal. This appears to be the only possible interpretation as the mining operation and the subsequent deposition of tailing material occur arbitrarily. The extracted material undergoes processing, and its subsequent deposition is characterized as arbitrary due to intermixing during both the processing and deposition phases of the mining operation.

Additionally, the interpretation of the stationarity results regarding tailing boreholes could potentially reveal that stationary boreholes (RJ-1 and RJ-3) exhibited comparatively uniform deposition, whereas the non-stationary borehole (RJ-2) demonstrated greater variability in material, as also evidenced by the highest CV parameter, suggesting episodic or mixed depositional processes. This interpretation may also be associated with possessing two ZI's, sharing one with both RJ-1 (4–6-meter ZI) and RJ-3 (10+ meter).

The results regarding the secondary objective of this research, which involves testing various time-series analysis methods for spatially-dependent data, are also ambiguous. The first-difference graph emphasizes areas of significant fluctuation in the x data; however, it does not convey supplementary information compared to the original data. The CUSUM graph offers a compelling method to visualize and monitor data fluctuations from the mean, demonstrating potential for further application in spatially-dependent datasets but further data is needed in order to completely gauge the effectiveness of the CUSUM graph. Finally, stationarity tests provide interesting results, indicating that the mean and variance remain constant across the spatial index of a dataset; however, additional research is necessary to confidently apply these tests to spatial data and to efficiently define the area where stationarity test can be best utilized.

The future possibilities for the broader application of MS and statistical methods in the characterization of tailing materials appear promising. The literature review demonstrated that the effective implementation of the MS method across various environmental contexts necessitating the spatial

distribution of heavy metals yielded promising outcomes in terms of cost efficiency and the time taken to produce results. The presented methodology may potentially reduce the sample range concerning geochemical and mineralogical analyses. This can be achieved by performing χ measurements to refine the geochemical and mineralogical samples to those exhibiting high χ values and statistical significance, indicating that the layer in question differs from neighboring layers.

5. Conclusion

This paper provides a statistical analysis of tailings material from three boreholes at the Rudnik mine in the Republic of Serbia, highlighting the identification and spatial distribution of heavy metals through magnetic susceptibility (MS) measurements. The research objectives were to assess the material similarity between boreholes, identify potential zones of elevated χ , and evaluate various statistical methods on spatially-dependent datasets.

The comparison and correlation of χ results among the three boreholes was difficult due to the heterogeneous and anthropogenic characteristics of the tailings deposits. Although localized areas of interest exhibited certain similarities, the data revealed a predominantly irregular and arbitrary deposition and distribution pattern. The optimal approach was to interpret the material as containing some locally similar zones of interest, yet being predominantly arbitrarily deposited.

Nonetheless, the statistical analysis effectively identified areas with heightened MS values with quantifiable confidence. These results establish a robust foundation for further focused geochemical and mineralogical studies, but more MS data is needed to further refine the methods and display the weaknesses and use cases in different situations.

The utilization of time-series analysis techniques on spatially-dependent data yielded interesting yet partial results. The first-difference transformation and visualization graph conveyed information that was also readily observable in the original dataset graph. The cumulative sum graph offered an innovative method to illustrate the dataset's fluctuations relative to a specified mean value and to highlight significant change points. Ultimately, stationarity tests may be beneficial in the future for assessing whether the dataset exhibits consistent statistical properties throughout the spatial domain and is potentially the most promising applied statistical method.

This study underscores the inherent complexity of tailings characterization and illustrates the utility of combining statistical and geophysical methods to identify economically and environmentally significant secondary resources in mining waste. Such methodologies facilitate more sustainable and informed practices in tailings management.

Mining tailings present considerable environmental challenges, but innovative strategies for repurposing tailings material offer a promising solution to transform mining waste into valuable resources. MS measurements provide a rapid, simple, and cost-effective technique for detecting the presence and distribution of heavy metals in tailings and thus future research will concentrate on further applying statistical tools to the MS measurements to gather more valuable information from the acquired data.

Acknowledgments – This research was supported by the Science Fund of the Republic of Serbia, Grant No. 7522- Characterisation and technological procedures for recycling and reusing of the Rudnik mine flotation tailings (REASONING). The authors would also like to thank Magdalena Marčeva and Simona Jevremović for their assistance during the acquisition and preparation of samples for magnetic susceptibility measurements. The authors would like to express their sincere gratitude to Rudnik and Flotation “Rudnik” d.o.o. Rudnik for permission to collect samples and for their cooperation during the research.

References

Abramović, F., Cvetkov, V., Ilić, A., and Životić, D. (2022): Correlation of magnetic susceptibility and content of metal in flotation tailings, XVIII Serbian Geological Congress, Divčibare, Republic of Serbia, 1–4 June 2022.

Ayoubi, S. and Mirsaldi, A. (2019): Magnetic susceptibility of Entisols and Aridisols great groups in southeastern Iran, *Geoderma Reg.*, 16, e00202, <https://doi.org/10.1016/j.geodrs.2018.e00202>

Barraza, F. P., Thiagarajan, D., Ramadoss, A., Manikandan, V. S., Dhanabalan, S. S., Venegas Abarzúa, C., Sotomayor Soloaga, P., Campos Nazer, J., Morel, M. J., and Thirumurugan, A. (2024): Unlocking the potential: Mining tailings as a source of sustainable nanomaterials. *Renewable and Sustainable Energy Reviews*, 197, 114665. <https://doi.org/10.1016/j.rser.2024.114665>

Bartington Instruments Ltd. (2008): Operation manual for MS2 magnetic susceptibility system, Bartington Instruments Ltd., Witney, UK, available at: <https://gmw.com/wp-content/uploads/2019/03/MS2-OM0408.pdf> (accessed: 6 December 2024).

Bityukova, L., Scholger, R., and Birke, M. (1999): Magnetic susceptibility as an indicator of environmental pollution of soils in Tallinn, *Phys. Chem. Earth A Solid Earth Geod.*, 24, 829–835, [https://doi.org/10.1016/S1464-1895\(99\)00122-2](https://doi.org/10.1016/S1464-1895(99)00122-2)

Bojko, T., Scholger, R., and Stanjek, H. (2004): Topsoil magnetic susceptibility mapping as a tool for pollution monitoring: repeatability of in situ measurements, *J. Appl. Geophys.*, 55, 249–259, <https://doi.org/10.1016/j.jappgeo.2004.01.002>

Briffa, J., Sinagra, E. and Blundell, R. (2020): Heavy metal pollution in the environment and their toxicological effects on humans. *Heliyon*, 6(9), e04691. <https://doi.org/10.1016/j.heliyon.2020.e04691>

Brempong, F., Mariam, Q., and Preko, K. (2016): The use of magnetic susceptibility measurements to determine pollution of agricultural soils in road proximity, *Afr. J. Environ. Sci. Technol.*, 10, 263–271, <https://doi.org/10.5897/ajest2015.2058>

Cacciuttolo, C., Cano, D., and Custodio, M. (2023): Socio-environmental risks linked with mine tailings chemical composition: promoting responsible and safe mine

tailings management considering copper and gold mining experiences from Chile and Peru, *Toxics*, **11**, 462, <https://doi.org/10.3390/toxics11050462>

Cardoso, D.O. and Galeno, T.D. (2023): Online evaluation of the Kolmogorov–Smirnov test on arbitrarily large samples. *J. Comput. Sci.*, **67**, 101959. <https://doi.org/10.1016/j.jocs.2023.101959>

Cvetković, V., Šarić, K., Pécskay, Z., and Gerdes, A. (2016): The Rudnik Mts. volcano-intrusive complex (central Serbia): an example of how magmatism controls metallogeny, *Geol. Croat.*, **69**, 89–99, <https://doi.org/10.4154/gc.2016.08>

D'Emilio, M., Caggiano, R., Coppola, R., Esposito, M., Giordano, S., and Ragosta, M. (2010): Magnetic susceptibility measurements as a proxy method to monitor soil pollution: the case study of S. Nicola di Melfi, *Environ. Monit. Assess.*, **169**, 619–630, <https://doi.org/10.1007/s10661-009-1201-5>

Dickey, D.A. and Fuller, W.A. (1979): Distribution of the estimators for autoregressive time series with a unit root, *J. Am. Stat. Assoc.*, **74**, 427–431, <https://doi.org/10.1080/01621459.1979.10482531>

Dickey, D.A. and Fuller, W.A. (1981): Likelihood ratio statistics for autoregressive time series with a unit root, *Econometrica*, **49**, 1057, <https://doi.org/10.2307/1912517>

Gómez-García, C., Martín-Hernández, F., García, J.Á.L., Ferrer, C., and Oyarzun, R. (2015): Rock magnetic characterization of the mine tailings in Portman Bay (Murcia, Spain) and its contribution to the understanding of the bay infilling process, *J. Appl. Geophys.*, **120**, 48–59, <https://doi.org/10.1016/j.jappgeo.2015.06.008>

Hanesch, M. and Scholger, R. (2002): Mapping of heavy metal loadings in soils by means of magnetic susceptibility measurements, *Environ. Geol.*, **42**, 857–870, <https://doi.org/10.1007/s00254-002-0604-1>

Hanesch, M. and Scholger, R. (2005): The influence of soil type on the magnetic susceptibility measured throughout soil profiles, *Geophys. J. Int.*, **161**, 50–56, <https://doi.org/10.1111/j.1365-246X.2005.02577.x>

Hartigan, J.A. and Hartigan, P.M. (1985): The dip test of unimodality, *Ann. Stat.*, **13**, <https://doi.org/10.1214/aos/1176346577>

Hyndman, R.J. and Athanasopoulos, G. (2021): *Forecasting: Principles and Practice* (3rd ed.). Monash University, Melbourne, Australia.

Jabłońska, M., Rachwał, M., Wawer, M., Kozłowska, A., and Cabała, J. (2021): Mineralogical and chemical specificity of dusts originating from iron and non-ferrous metallurgy in the light of their magnetic susceptibility, *Minerals*, **11**, 216, <https://doi.org/10.3390/min11020216>

Jaffar, S.T.A., Chen, L.-Z., Younas, H., and Ahmad, N. (2017): Heavy metals pollution assessment in correlation with magnetic susceptibility in topsoils of Shanghai, *Environ. Earth Sci.*, **76**, <https://doi.org/10.1007/s12665-017-6598-5>

Jain, P. K., Mandre, N. R., and Bhattacharya, S. (2025): Flotation. In *Treatise on Process Metallurgy, Volume 2B*, 131–145. Elsevier.

Jaishankar, M., Tseten, T., Anbalagan, N., Mathew, B.B. and Beeregowda, K.N. (2014): Toxicity, mechanism and health effects of some heavy metals. *Interdiscip. Toxicol.*, **7**(2), 60–72. <https://doi.org/10.2478/intox-2014-0009>

Jawadand, S., and Randive, K. (2021): A sustainable approach to transforming mining waste into value-added products. In *Innovations in Sustainable Mining: Balancing Environment, Ecology and Economy*, 1–20. Springer International Publishing, Cham, Switzerland.

Jelenković, R., Kostić, A., Životić, D., and Ercegovac, M. (2008): Mineral resources of Serbia, *Geol. Carpath.*, **59**(4), 345–361.

Jordanova, D., Goddu, S.R., Kotsev, T., and Jordanova, N. (2013): Industrial contamination of alluvial soils near Fe–Pb mining site revealed by magnetic and geochemical studies, *Geoderma*, **192**, 237–248, <https://doi.org/10.1016/j.geoderma.2012.07.004>

Karimi, R., Ayoubi, S., Jalalian, A., Honarjoo, N., and Alavipanah, S.K. (2011): Relationships between magnetic susceptibility and heavy metals in urban topsoils in the arid region of Isfahan, central Iran, *J. Appl. Geophys.*, **74**, 1–7, <https://doi.org/10.1016/j.jappgeo.2011.02.009>

Kim, J. G., Park, J. S., Chon, C. M., and Lee, Y. S. (2010): Relationship between magnetic susceptibility and heavy metal content of soil, in 19th World Congress of Soil Science, Soil Solutions for a Changing World, pp. 1–6.

Kwiatkowski, D., Phillips, P.C.B., Schmidt, P., and Shin, Y. (1992): Testing the null hypothesis of stationarity against the alternative of a unit root, *J. Econom.*, **54**, 159–178, [https://doi.org/10.1016/0304-4076\(92\)90104-Y](https://doi.org/10.1016/0304-4076(92)90104-Y)

Lam, E.J., Carle, R., González, R., Montofré, I.L., Veloso, E.A., Bernardo, A., Cánovas, M., and Álvarez, F.A. (2020): A methodology based on magnetic susceptibility to characterize copper mine tailings, *Minerals*, **10**, 939, <https://doi.org/10.3390/min10110939>

Lecoanet, H., Lévéque, F., and Segura, S. (1999): Magnetic susceptibility in environmental applications: comparison of field probes, *Phys. Earth Planet. Inter.*, **115**, 191–204, [https://doi.org/10.1016/S0031-9201\(99\)00066-7](https://doi.org/10.1016/S0031-9201(99)00066-7)

Rodgers, J. and Nicewander, W.A. (1988): Thirteen ways to look at the correlation coefficient, *Am. Stat.*, **42**(1), 59–66.

Liu, D., Liu, Z., Wang, Y., and Zhou, L. (2023): Editorial: Understanding heavy metal pollution and control in the environment around metal tailings, *Front. Environ. Sci.*, **11**, <https://doi.org/10.3389/fenvs.2023.1168949>

Lyocsa, S., Vyrost, T., and Baumohl, E. (2011): Unit-root and stationarity testing with empirical application on industrial production of CEE-4 countries, *SSRN Electron. J.*, <https://doi.org/10.2139/ssrn.1785223>

Morales, J., Del Sol Hernández-Bernal, M., Corona-Chávez, P., Hernández-Álvarez, E., and Flores-Márquez, E.L. (2016): Further evidence for magnetic susceptibility as a proxy for the evaluation of heavy metals in mining wastes: case study of Tlalpujahua and El Oro Mining Districts, *Environ. Earth Sci.*, **75**, <https://doi.org/10.1007/s12665-015-5187-8>

Naimi, S. and Ayoubi, S. (2013): Vertical and horizontal distribution of magnetic susceptibility and metal contents in an industrial district of central Iran, *J. Appl. Geophys.*, **96**, 55–66, <https://doi.org/10.1016/j.jappgeo.2013.06.012>

Nenes, G. and Tagaras, G. (2006): The economically designed CUSUM chart for monitoring short production runs, *Int. J. Prod. Res.*, **44**, 1569–1587, <https://doi.org/10.1080/00207540500422197>

Nišić, D., Aleksić, N., Živanović, B., Jovanović, M., Mitić, V., and Marković, S. (2024): Review of the failure at the flotation tailings storage facility of the “Stolice” Mine (Serbia), *Appl. Sci.*, **14**, 10163, <https://doi.org/10.3390/app142210163>

Obrenović, L., Mladenović, M., and Janić, S. (2025): Plan upravljanja rudarskim otpadom rudnika Rudnik [Mining waste management plan of the Rudnik Mine]. Internal report in Serbian, 169 pp. Rudnik.

Oudeika, M.S., Altinoglu, F.F., Akbay, F., and Aydin, A. (2020): The use of magnetic susceptibility and chemical analysis data for characterizing heavy metal contamination of topsoil in Denizli city, Turkey, *J. Appl. Geophys.*, **183**, 104208, <https://doi.org/10.1016/j.jappgeo.2020.104208>

Petrović, S., Bakker, R.J., Cvetković, V., and Jelenković, R. (2024): Multiphase evolution of fluids in the Rudnik hydrothermal-skarn deposit (Serbia): new constraints from study of quartz-hosted fluid inclusions, *Mineral. Petrol.*, **118**, 461–482, <https://doi.org/10.1007/s00710-024-00860-7>

Petrovský, E., Kapička, A., Jordanova, N., and Knab, M. (2000): Low-field magnetic susceptibility: a proxy method of estimating increased pollution of different environmental systems, *Environ. Geol.*, **39**, 312–318, <https://doi.org/10.1007/s002540050010>

Popović, R. and Umeljić, G. (2015): Metallogeny of the Rudnik mountain, position in time and space [Original title: Metalogenija planine Rudnik, pozicija u vremenu i prostoru], *Povremena izdanja Rudnik i flotacija 'Rudnik' doo Rudnik*, Beograd, 224 pp., ISBN 978-86-918511-0-1 [In Serbian].

Salehi, M.H., Jorkesh, S., and Mohajer, R. (2013): Relationship between magnetic susceptibility and heavy metals concentration in polluted soils of Lenjanat Region, Isfahan, E3S Web Conf., 1, 04003, <https://doi.org/10.1051/e3sconf/20130104003>

Schober, P., Boer, C., and Schwarte, L.A. (2018): Correlation coefficients: appropriate use and interpretation, *Anesth. Analg.*, **126**, 1763–1768, <https://doi.org/10.1213/ane.00000000000002864>

Stojanović, J., Radosavljević, S., Tošović, R., Petrović, S., and Životić, D. (2018): A review of the Pb–Zn–Cu–Ag–Bi–W polymetallic ore from the Rudnik orefield, central Serbia, *Geol. An. Balk. Pol.*, **79**, 47–69, <https://doi.org/10.2298/gabp1879047s>

Stojanović, J., Radosavljević-Mihajlović, A., Radosavljević, S., and Petrović, S. (2016): Mineralogy and genetic characteristics of the Rudnik Pb–Zn/Cu,Ag,Bi,W polymetallic deposit (central Serbia): new occurrence of Pb(Ag)Bi sulfosalts, *Period. Mineral.*, **85**, <https://doi.org/10.2451/2016pm605>

Su, C., Rana, N.M., Zhang, S., and Wang, B. (2024): Environmental pollution and human health risk due to tailings storage facilities in China, *Sci. Total Environ.*, **928**, 172437, <https://doi.org/10.1016/j.scitotenv.2024.172437>

Tchounwou, P.B., Yedjou, C.G., Patlolla, A.K. and Sutton, D.J. (2012): Heavy metal toxicity and the environment. *Exp. Suppl.*, **101**, 133–164. https://doi.org/10.1007/978-3-7643-8340-4_6

Vasiliev, A., Gorokhova, S., and Razinsky, M. (2020): Technogenic magnetic particles in soils and ecological–geochemical assessment of the soil cover of an industrial city in the Ural, Russia, *Geosci.*, **10**, 443, <https://doi.org/10.3390/geosciences10110443>

Velicer, W.F. and Fava, J.L. (2003): Time series analysis. In: Weiner, I.B. (ed.), *Handbook of Psychology*. Wiley, New York, USA. <https://doi.org/10.1002/0471264385.wei0223>

Wang, X.S. (2013): Assessment of heavy metal pollution in Xuzhou urban topsoils by magnetic susceptibility measurements, *J. Appl. Geophys.*, **92**, 76–83, <https://doi.org/10.1016/j.jappgeo.2013.02.015>

Wawer, M. (2020): Identification of technogenic magnetic particles and forms of occurrence of potentially toxic elements present in fly ashes and soil, *Minerals*, **10**, 1066, <https://doi.org/10.3390/min10121066>

Yurtseven-Sandker, A. and Cioppa, M.T. (2016): Tracking the historical traces of soil pollution from an iron-sintering plant by using magnetic susceptibility in Wawa, Ontario, Canada, *Water Air Soil Pollut.*, **227**, <https://doi.org/10.1007/s11270-016-3140-4>

Zar, J.H. (2005): Spearman rank correlation, in *Encyclopedia of Biostatistics*, eds P. Armitage and T. Colton, Wiley, <https://doi.org/10.1002/0470011815.b2a15150>

Zawadzki, J., Fabijańczyk, P., Magiera, T., and Rachwał, M. (2015): Geostatistical microscale study of magnetic susceptibility in soil profile and magnetic indicators of potential soil pollution, *Water Air Soil Pollut.*, **226**, <https://doi.org/10.1007/s11270-015-2395-5>

SAŽETAK

Statistička analiza varijacija magnetske susceptibilnosti u flotacijskoj jalovini rudnika Rudnik, Republika Srbija

*Filip Arnaut, Vesna Cvetkov, Stefan Petrović, Nikola Stanković,
Vladimir Simić i Dimitry Sidorov Biryukov*

Rudničke jalovine sve se više prepoznaju kao potencijalno vrijedni izvori mineralnih sirovina. Ovo istraživanje primjenjuje analizu magnetske susceptibilnosti na tri bušotine u flotacijskom jalovištu s odlagališta rudnika olova i cinka Rudnik u Srbiji. Uzorci su prikupljeni na malim prostornim razmacima (10 cm), što je omogućilo primjenu različitih statističkih metoda na dobivenom skupu podataka. Rezultati pokazuju da se međusobna sličnost između bušotina ne može statistički značajno utvrditi; međutim, odredene zone između bušotina pokazuju odredene sličnosti. Te varijacije se pripisuju antropogenom deponiranju, gdje su lokalni materijali bili izmiješani i nasumično odlagani tokom eksplotacije i prerade, što onemogućava jasne statističke korelacije. Studija identificira ključne zone od interesa u sve tri bušotine za dalja geokemijska i mineraloška istraživanja.

Ključne riječi: Prostorna analiza, magnetski susceptibilitet, antropogeno taloženje, geostatistika, jalovina, recikliranje jalovine

Corresponding author's address: Filip Arnaut, Institute of Physics Belgrade, University of Belgrade, Pregrevica 118, Belgrade, Republic of Serbia. email: filip.arnaut@ipb.ac.rs.



This work is licensed under a [Creative Commons Attribution-NonCommercial 4.0 International License](https://creativecommons.org/licenses/by-nc/4.0/).